



Published in final edited form as:

J Cataract Refract Surg. 2006 November ; 32(11): 1836–1842.

High-speed Optical Coherence Tomography for Management after Laser in Situ Keratomileusis

Mariana Avila, MD, Yan Li, MS, Jonathan C. Song, MD, and David Huang, MD, PhD

Doheny Eye Institute and Department of Ophthalmology, Keck School of Medicine of the University of Southern California, Los Angeles, California, USA.

Abstract

PURPOSE: To report applications of optical coherence tomography (OCT) in the management of laser in situ keratomileusis (LASIK) related problems.

SETTING: Doheny Eye Institute and Department of Ophthalmology, Keck School of Medicine of the University of Southern California, Los Angeles, California, USA.

METHODS: Five patients referred for LASIK-related problems were enrolled in a prospective observational study. Clinical examination, ultrasound (US) pachymetry, Placido ring slit-scanning corneal topography (Orbscan II, Bausch & Lomb), and high-speed corneal OCT were performed.

RESULTS: In cases of regression and keratectasia, OCT provided thickness measurements of the cornea, flap, and posterior stromal bed. Locations of tissue loss and flap interface planes were identified in a case with a recut enhancement complication. The information was used to determine whether further laser ablation was safe, confirm keratectasia, and manage complications. Optical coherence tomography measurements of central corneal thickness agreed well with US pachymetry measurements (difference 6.4 mm G 11.7 [SD]) (P Z .026), while Orbscan significantly underestimated corneal thickness ($-67.5 \pm 72.5 \mu\text{m}$) (P = .17).

CONCLUSIONS: High-speed OCT provided noncontact imaging and measurement of LASIK anatomy. It was useful in monitoring LASIK results and evaluating complications.

Laser in situ keratomileusis (LASIK) is an effective procedure for a wide range of refractive errors when performed within the proper anatomic guidelines.¹⁻⁵ A well-accepted guideline is the requirement to preserve adequate posterior corneal stromal thickness to reduce the risk for keratectasia.^{2,6-9}

Several tools help the refractive surgeon measure corneal anatomy. Ultrasound (US) pachymetry is commonly used to measure the central corneal thickness. Intraoperative US pachymetry can also provide measurements of stromal bed thickness and, by subtraction, measurements of flap thickness.¹⁰⁻¹² Ultrasound pachymetry is limited because it provides only a single spot measurement and the precision of probe placement is approximate. Slit-scanning corneal tomography provides corneal thickness mapping, but it cannot measure the thickness of the flap and stromal bed. Ultrasound imaging can map post-LASIK corneal layers,¹³⁻¹⁵ but the technique is not commonly used because it requires a cumbersome waterbath.

Corresponding author: David Huang, MD, PhD, 1450 San Pablo Street, DEI 5702, Los Angeles, California 90033, USA. E-mail: dhuang@usc.edu.

Supported by grants from NIH (R01 EY013516 and P30 EY03040), Research to Prevent Blindness, Inc., and Carl Zeiss Meditec, Inc.

Dr. Huang has a patent royalty interest in optical coherence tomography technology. Drs. Huang and Li receive research grant support from Carl Zeiss Meditec Inc. Drs. Avila and Song have no financial or proprietary interest in any material or method mentioned.

Therefore, a quick and noncontact corneal imaging technology to map corneal layers is still needed.¹⁶

Optical coherence tomography (OCT)¹⁷ is a noncontact imaging technology that provides cross-sectional images of the cornea from which thickness measurements can be taken. The first published corneal OCT image was shown by Izatt et al.¹⁸ in 1994, and a study of LASIK flap-thickness measurement with OCT was published by Maldonado et al.¹⁹ in 2000. These and several other earlier efforts²⁰⁻²⁴ used relatively slow OCT scanners that were not suitable for mapping or profiling a large area of the cornea. Our research group has worked with academic and industry partners to develop high-speed OCT systems that can profile and map the cornea. The key improvements include a longer wavelength (relative to retinal OCT) of 1.3 μm for safe use of higher incident power and faster scanning^{25,26} and telecentric scanning to provide undistorted imaging over a wide area.²⁵⁻²⁷

This case series report demonstrates the usefulness of high-speed corneal and anterior segment (CAS-OCT) technology in the management of LASIK problems.

PATIENTS AND METHODS

Five patients who returned for follow-up or were referred for consultation for post-LASIK management issues were evaluated at the Doheny Laser Vision Center. Informed consent was obtained from all participants, and the study was reviewed by the Institutional Review Board of Doheny Eye Institute. Optical coherence tomographic imaging of the cornea and anterior segment was performed under a prospective observations study protocol approved by the Institutional Review Board of the University of Southern California. The study adhered to the tenets of the Declaration of Helsinki. Clinical history, slitlamp examination, US pachymetry, and Placido ring slit-scanning corneal topography (Orbscan II, Bausch & Lomb, Inc.) were also performed as part of the study.

The CAS-OCT prototype was provided by Carl Zeiss Meditec, Inc. The system has a speed of 2000 axial scans (A-scans) per second and a telecentric scan geometry. (The OCT beam remains parallel to the central optical axis as it is scanned transversely.) The patient's head was stabilized with a chin rest. The patient's gaze was fixed with a pie-chart style internal fixation target with the apparent fixation distance adjusted to the eye's spherical equivalent refraction. The OCT and video camera images were displayed in real time to aid alignment. The center of the scan pattern was aligned with the corneal vertex reflection visualized on the OCT images. Two scan patterns were used, one to provide a corneal pachymetry map and the other to provide detailed cross-sectional images and compute thickness profiles. The pachymetry map pattern is composed of radial lines on 8 evenly spaced meridians arranged in a spoke-like pattern. The pattern covers a 10.0 mm diameter area centered on the corneal vertex reflection. Each meridional line contains 128 A-scans. The flap profile pattern is an 8.0 mm long horizontal line that contains 512 A-scans. Four consecutive frames were saved for each scan. The data acquisition time was 0.5 second for the pachymetry map pattern and 1 second for the flap profile pattern. The A-scans spanned 4.0 mm in depth. Three OCT scans of each scan pattern of each eye were obtained by the same photographer. The patient was repositioned after each scan.

The OCT images were exported and processed using custom software. The consecutive frames of the flap profile scans were registered to remove frame-to-frame motion error and then averaged. The averaging removes speckle and increases signal-to-noise ratio, making measurements more reliable. The images were first "dewarped" to eliminate the distortions caused by refraction and group index transition at the air-cornea interface. The anterior and posterior corneal boundaries and the flap interface were identified by automated computer

algorithms. The accuracy of the algorithms to measure corneal thickness²⁸ and flap thickness have been validated by comparison with US measurements (Huang D, et al. IOVS 2005; 46:ARVO E-Abstract 1077). Corneal, flap, and posterior stromal bed thicknesses were measured along lines perpendicular to the anterior surface. These thicknesses were plotted on a profile and color-coded maps.

Table 1 summarizes the OCT flap and posterior stromal bed thickness measurements at the corneal center and the key conclusions.

RESULTS

Case 1

A 56-year-old man was referred by the primary LASIK surgeon to rule out keratectasia. He had wavefront-guided LASIK for myopia correction in both eyes 6 months previously and had a progressive myopic shift that required spectacle correction. Enhancement in the right eye was scheduled but canceled because an Orbscan image showed an abnormal posterior elevation map suspicious for keratectasia (Figure 1,A). The map showed an elevated spot inferocentrally that was 56 mm above the best-fit sphere. There was no risk factor for keratectasia before the LASIK surgery, and the preoperative corneal topography was normal. Pre-LASIK US pachymetry was 573 mm in the right eye and 581 mm in the left eye. The Hansatome was used with a 180 mm depth setting. Ablation depth was 88 mm in the right eye and 69 mm in the left eye.

The uncorrected visual acuity (UCVA) was 20/40 in the right eye and 20/60 in the left eye. The manifest refraction was $-1.00 + 0.25 \times 30$ (20/20) and $-1.25 + 0.25 \times 105$ (20/15), respectively. The slitlamp examination was normal. Ultrasound central pachymetry was 532 mm in the right eye and 550 mm in the left eye. Orbscan anterior topography was normal (Figure 1,A).

The OCT profile scans of the right eye (Figure 1,B) and left eye showed normal central thickness on the corneal, flap, and stromal bed scans (Table 1).

In the absence of any abnormality on the anterior topography, it was not believed that the increased posterior elevation on Orbscan indicated keratectasia. The OCT measurement showed sufficient residual posterior stroma for further laser ablation to correct the residual myopia, and the enhancement was performed. Three months after the enhancement, the patient reported good quality of vision. Manifest refraction was C0.25 sphere (20/20) in the right eye and plano (20/20) in the left eye. There was no sign of ectasia on corneal topography and slitlamp examination.

Case 2

A 48-year-old woman was referred for evaluation of decreased vision and flap interface haze in the left eye after myopic LASIK and 3 enhancements over a span of 4 years. Diffuse lamellar keratitis was noted after one of the enhancements.

The UCVA in the left eye was 20/40. Manifest refraction was $-1.00 + 0.75 \times 60$ (20/40⁻²). With rigid gaspermeable lens (RGP) overrefraction, acuity improved to 20/20. Slitlamp examination of the cornea showed a layer of fine granular haze at the flap interface centrally, moderate mud-crack microstriae, a few spots of scarring in the periphery at the 4 to 5 o'clock position, and mild inferior punctate epithelial erosion. All four Orbscan maps showed signs of keratectasia (Figure 2,A). The anterior axial power map showed a skewed asymmetric bow tie with inferior steepening. The anterior mean power (curvature) map, posterior elevation map, and corneal

thickness map showed an inferotemporal spot of abnormally increased convexity, elevation, and thinning, respectively.

The OCT profile scan of the left eye (Figure 2,B) showed a central flap thickness of 217 μm and an abnormally thin stromal bed thickness of 244 μm . The unusually thick flap helped cause the thin residual stromal bed. The patient was advised against further laser enhancement in the left eye, and RGP contact lens correction was recommended.

Case 3

A 63-year-old man was referred for visual problems in the left eye after LASIK, cataract surgery, and LASIK enhancements in both eyes. Examination, including corneal topography, showed secondary myopia in the left eye without evidence of keratectasia. The OCT measurements showed sufficient residual posterior stromal thickness for further myopic ablation (Table 1). Wavefront-guided LASIK retreatment led to a final UCVA of 20/20.

Case 4

A 43-year-old man was referred for evaluation of keratectasia after LASIK. With spectacle correction, visual acuity was 20/30 with $-3.50 + 5.50 \times 173$ in the right eye and 20/25⁻¹ with $-4.50 + 6.50 \times 19$ in the left eye. With pinhole, visual acuity was 20/20⁻¹ and 20/20⁻¹, respectively. Orbscan anterior and posterior topographies showed signs of keratectasia in both eyes.

The OCT measurements showed normal central thickness on corneal, flap, and stromal bed scans (Table 1). Thus, insufficient residual stromal bed thickness was not a risk factor for keratectasia in this case. This patient probably had forme fruste keratoconus before LASIK. The pre-LASIK topography for confirmation could not be obtained.

The patient was advised against laser retreatment. He elected to wear RGP contact lenses in both eyes and later had intrastromal corneal ring implantation in the right eye.

Case 5

A 52-year-old woman was referred for a flap recut complication during enhancement for residual myopia in the left eye. A loose sliver of tissue was noted when the flap was reflected. The tissue was removed because its original location was uncertain. The flap was replaced, and no enhancement ablation was performed. The patient reported poor vision in the left eye after the complication.

One month after the complication, the UCVA in the left eye was 20/200. The manifest refraction was $+5.00 - 1.50 \times 180$ (20/50). With RGP overrefraction, acuity was 20/25. Orbscan of the left eye showed irregular anterior topography.

An OCT profile scan (Figure 3,A) showed two flap interfaces that intersected temporally. The single interface in the temporal periphery was consistent with loss of a tissue lenticule from the flap. Residual stromal bed thickness was 291 μm centrally. The OCT corneal thickness map (Figure 3,B) confirmed that the loss of tissue was centered approximately 1.5 mm temporally. The patient was intolerant of an RGP contact lens and opted to have surgical correction. She was referred for photorefractive keratectomy (PRK) with TopoLink using an Allegretto laser (WaveLight) at a Canadian center, after which UCVA was improved to 20/30.

Optical Coherence Tomography Versus Orbscan Pachymetry

Table 2 compares the total central corneal thickness measurements by OCT, US pachymetry, and Orbscan. Orbscan significantly underestimated central corneal thickness compared to US ($P = .026$, t test). The OCT measurements agreed with US pachymetry measurements.

Axial scans from similar locations in a normal eye (without LASIK) were acquired using the OCT system and the Orbscan II system and compared (Figure 4). The OCT A-scan showed distinct signal peaks at the air-tear interface and the cornea-aqueous interface (Figure 4,A). In the Orbscan II A-scan plot (Figure 4,B), the stromal signal was stronger and there were no distinct signal peaks corresponding to the anterior and posterior surface reflections.

DISCUSSION

In this series, we found OCT a useful adjunct to corneal topography for the evaluation of post-LASIK problems. Optical coherence tomography provides non-contact measurement of the flap and posterior stromal bed thickness. This measurement is particularly valuable for confirming there is an adequate residual stromal bed before enhancement ablations for regression and under correction are performed. Although intraoperative US measurement of the stromal bed during primary LASIK could provide similar information, it is not always measured and is often not available. Furthermore, OCT measurement just before enhancement provides more immediate confirmation that no thinning of the posterior stromal bed has occurred as a result of keratectasia after the previous surgery. The finding of an abnormally thin posterior stromal bed thickness on OCT provides an explanation for the cause of the keratectasia and supports the diagnosis. Routine use of OCT in the longitudinal follow-up of LASIK could also provide screening for early keratectasia. We performed a longitudinal OCT study of normal post-LASIK corneal anatomy (Huang D, et al. IOVS 2005; 46:ARVO E-Abstract 1077) and will publish the findings in a separate article.

Optical coherence tomography provides a corneal thickness map similar to that available from slit-scanning tomography techniques such as the Orbscan and Pentacam (Oculus Optikgerate GmbH). In this series, OCT pachymetry agreed well with US pachymetry, while Orbscan significantly underestimated central corneal thickness in post-LASIK eyes. Orbscan is known to systematically underestimate corneal thickness after LASIK and PRK.^{29,30} This is probably a result of the increased anterior stromal haze and modified anterior topography. According to the Orbscan II manual, the anterior and posterior boundaries are identified by the point of greatest gradient (slope). Looking at the Orbscan A-scan (Figure 4,B), one can understand why this is necessary because the Orbscan signal does not show distinct peaks at the corneal surfaces. Increased scattering from the flap or interface may skew the gradient measurement in Orbscan pachymetry. On the other hand, the OCT A-scan shows distinct signal peaks at the anterior and posterior corneal boundaries. Because of OCT's high spatial resolution, the interface peaks are well separated from stromal reflections. This allows accurate measurement regardless of corneal opacities. In separate studies, we showed that OCT corneal thickness measurement agrees closely with US pachymetry in normal eyes²⁸ and in eyes with corneal scars (Khurana RN, et al. IOVS 2006; 47:ARVO E-Abstract 1325). This robust pachymetric mapping capability is a major strength of corneal OCT. This is well illustrated in Case 5, in which the location of the missing flap lenticule is precisely shown in both the transverse (Figure 3,B) and depth (Figure 3,A) dimensions.

The underestimation of corneal thickness may be a reason Orbscan showed increased posterior topographic elevation after LASIK. This finding led the referring physician to suspect keratectasia in Case 1. Use of OCT can ensure there is no keratectasia (Case 1) or confirm and provide a causative explanation for keratectasia (Case 2).

Orbscan remains valuable for the diagnosis of keratoconus and keratectasia because it can map both the front and back corneal surfaces. We are working on software to measure the posterior corneal curvature with OCT. The initial clinical results are presented separately.³¹

The U.S. Food and Drug Administration recently approved a commercial high-speed CAS-OCT system (Visante OCT System, Carl Zeiss Meditec, Inc.) similar to the prototype tested in this study. This makes it possible for clinicians in the United States to use this technology to routinely monitor LASIK results.

Our case series shows the applications of OCT in the evaluation and management of select post-LASIK problems. We now routinely use OCT to plan LASIK enhancement procedures to ensure the patient has sufficient residual posterior stroma for the planned ablation. Although we rarely perform recut enhancement at our center, OCT measurement of flap depth is useful for selecting the recut depth as well. Routine use of OCT to follow the corneal anatomy after LASIK would also help monitor the performance of a microkeratome in terms of flap reproducibility and uniformity and would provide surveillance for potential cases of keratectasia.

REFERENCES

1. Pallikaris IG, Papatzanaki ME, Stathi EZ, et al. Laser in situ keratomileusis. *Lasers Surg Med* 1990;10:463–468. [PubMed: 2233101]
2. Pallikaris IG, Papatzanaki ME, Siganos DS, Tsilimbaris MK. A corneal flap technique for laser in situ keratomileusis; human studies. *Arch Ophthalmol* 1991;109:1699–1702. [PubMed: 1841579]
3. Pallikaris IG, Siganos DS. Excimer laser in situ keratomileusis and photorefractive keratectomy for correction of high myopia. *J Refract Corneal Surg* 1994;10:498–510. [PubMed: 7530099]
4. Stulting RD, Lahners WJ, Carr JD. Advances in refractive surgery; 1975 to the present. *Cornea* 2000;19:741–753. [PubMed: 11009326]
5. Sugar A, Rapuano CJ, Culbertson WW, et al. Laser in situ keratomileusis for myopia and astigmatism: safety and efficacy. (Ophthalmology Technology Assessment) A report by the American Academy of Ophthalmology. *Ophthalmology* 2002;109:175–187. [PubMed: 11772601]
6. Ou RJ, Shaw EL, Glasgow BJ. Keratectasia after laser in situ keratomileusis (LASIK): evaluation of the calculated residual stromal bed thickness. *Am J Ophthalmol* 2002;134:771–773. [PubMed: 12429260]
7. Seiler T, Koufala K, Richter G. Iatrogenic keratectasia after laser in situ keratomileusis. *J Refract Surg* 1998;14:312–317. [PubMed: 9641422]
8. Spadea L, Palmieri G, Mosca L, et al. Iatrogenic keratectasia following laser in situ keratomileusis. *J Refract Surg* 2002;18:475–480. [PubMed: 12160161]
9. Stulting RD, Carr JD, Thompson KP, et al. Complications of laser in situ keratomileusis for the correction of myopia. *Ophthalmology* 1999;106:13–20. [PubMed: 9917775]
10. Muallem MS, Yoo SH, Romano AC, et al. Flap and stromal bed thickness in laser in situ keratomileusis enhancement. *J Cataract Refract Surg* 2004;30:2295–2302. [PubMed: 15519078]
11. Nagy ZZ, Suveges I, Nemeth J. Intraoperative pachymetry during excimer photorefractive keratectomy. *Acta Chir Hung* 1995;1996:35–217.
12. Villaseñor RA, Santos VR, Cox KC, et al. Comparison of ultrasonic corneal thickness measurements before and during surgery in the Prospective Evaluation of Radial Keratotomy (PERK) Study. *Ophthalmology* 1986;93:327–330. [PubMed: 3517739]
13. Reinstein DZ, Silverman RH, Raevsky T, et al. Arc-scanning very high-frequency digital ultrasound for 3D pachymetric mapping of the corneal epithelium and stroma in laser in situ keratomileusis. *J Refract Surg* 2000;16:414–430. [PubMed: 10939721]
14. Reinstein DZ, Silverman RH, Rondeau MJ, Coleman DJ. Epithelial and corneal thickness measurements by high-frequency ultrasound digital signal processing. *Ophthalmology* 1994;101:140–146. [PubMed: 8302547]

15. Reinstein DZ, Silverman RH, Sutton HFS, Coleman DJ. Very high-frequency ultrasound corneal analysis identifies anatomic correlates of optical complications of lamellar refractive surgery; anatomic diagnosis in lamellar surgery. *Ophthalmology* 1999;106:474–482. [PubMed: 10080202]
16. Huang D. A reliable corneal tomography system is still needed [guest editorial]. *Ophthalmology* 2003;110:455–456. [PubMed: 12623804]
17. Huang D, Swanson EA, Lin C-P, et al. Optical coherence tomography. *Science* 1991;254:1178–1181. [PubMed: 1957169]
18. Izatt JA, Hee MR, Swanson EA, et al. Micrometer-scale resolution imaging of the anterior eye in vivo with optical coherence tomography. *Arch Ophthalmol* 1994;112:1584–1589. [PubMed: 7993214]
19. Maldonado MJ, Ruiz-Oblitas L, Munuera JM, et al. Optical coherence tomography evaluation of the corneal cap and stromal bed features after laser in situ keratomileusis for high myopia and astigmatism. *Ophthalmology* 2000;107:81–87. [PubMed: 10647724]discussion by DR Hardten, 88
20. Thompson RW Jr, Choi DM, Price MO, et al. Noncontact optical coherence tomography for measurement of corneal flap and residual stromal bed thickness after laser in situ keratomileusis. *J Refract Surg* 2003;19:507–515. [PubMed: 14518739]
21. Ustundag C, Bahcecioglu H, Ozdamar A, et al. Optical coherence tomography for evaluation of anatomical changes in the cornea after laser in situ keratomileusis. *J Cataract Refract Surg* 2000;26:1458–1462. [PubMed: 11033391]
22. Wang J, Thomas J, Cox I, Rollins A. Noncontact measurements of central corneal epithelial and flap thickness after laser in situ keratomileusis. *Invest Ophthalmol Vis Sci* 2004;45:1812–1816. [PubMed: 15161844]
23. Wirbelauer C, Pham DT. Continuous monitoring of corneal thickness changes during LASIK with online optical coherence pachymetry. *J Cataract Refract Surg* 2004;30:2559–2568. [PubMed: 15617925]
24. Wirbelauer C, Pham DT. Monitoring corneal structures with slitlampadapted optical coherence tomography in laser in situ keratomileusis. *J Cataract Refract Surg* 2004;30:1851–1860. [PubMed: 15342046]
25. Huang D, Li Y, Radhakrishnan S. Optical coherence tomography of the anterior segment of the eye. *Ophthalmol Clin North Am* 2004;17(1):1–6. [PubMed: 15102509]
26. Radhakrishnan S, Rollins AM, Roth JE, et al. Real-time optical coherence tomography of the anterior segment at 1310 nm. *Arch Ophthalmol* 2001;119:1179–1185. [PubMed: 11483086]
27. Huang, D.; Li, Y.; Radhakrishnan, S.; Chalita, MR. Corneal and anterior segment optical coherence tomography. In: Schuman, JS.; Puliafito, CA.; Fujimoto, JG., editors. *Optical Coherence Tomography of Ocular Dis-eases*. 2nd ed.. Slack; Thorofare, NJ: 2004. p. 663-673.
28. Li Y, Shekhar R, Huang D. Corneal pachymetry mapping with high-speed optical coherence tomography. *Ophthalmology* 2006;113:792–799. [PubMed: 16650675]
29. Chakrabarti HS, Craig JP, Brahma A, et al. Comparison of corneal thickness measurements using ultrasound and Orbscan slit-scanning topography in normal and post-LASIK eyes. *J Cataract Refract Surg* 2001;27:1823–1828. [PubMed: 11709257]
30. Prisant O, Calderon N, Chastang P, et al. Reliability of pachymetric measurements using Orbscan after excimer refractive surgery. *Ophthalmology* 2003;110:511–515. [PubMed: 12623813]
31. Tang M, Li Y, Avila M, Huang D. Measurement of total corneal power before and after LASIK with high-speed optical coherence tomography. *J Cataract Refract Surg*. In press

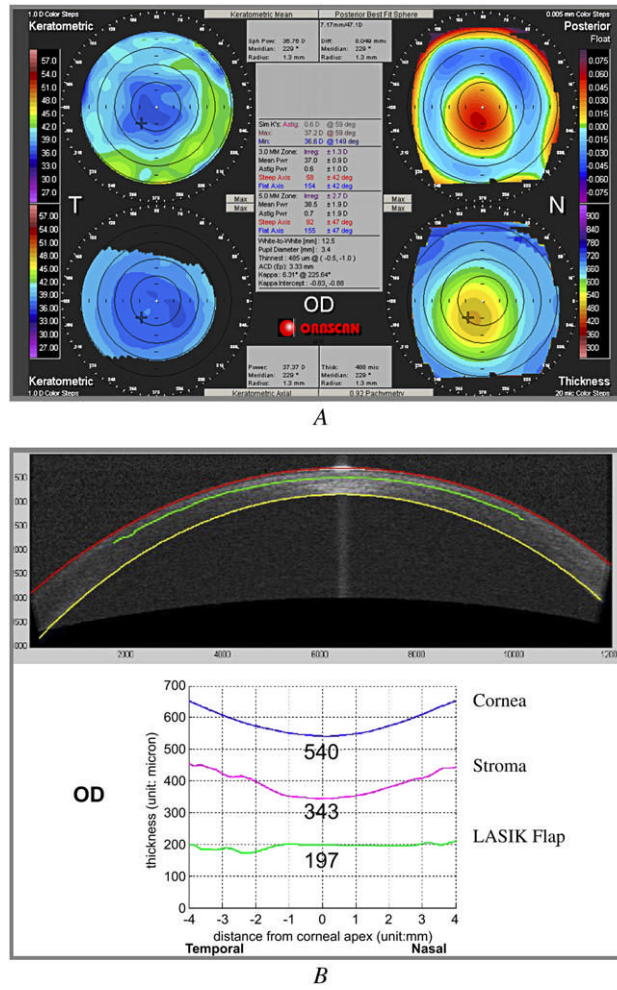
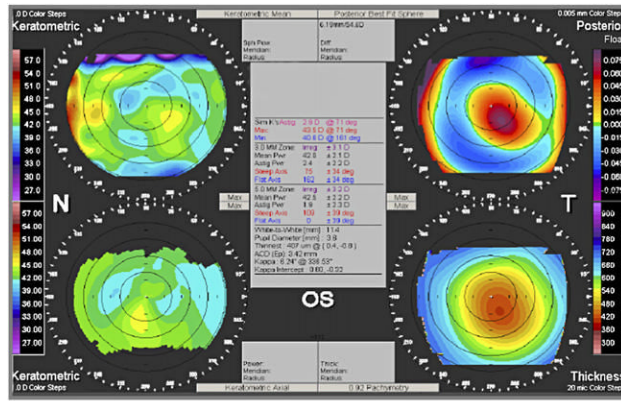
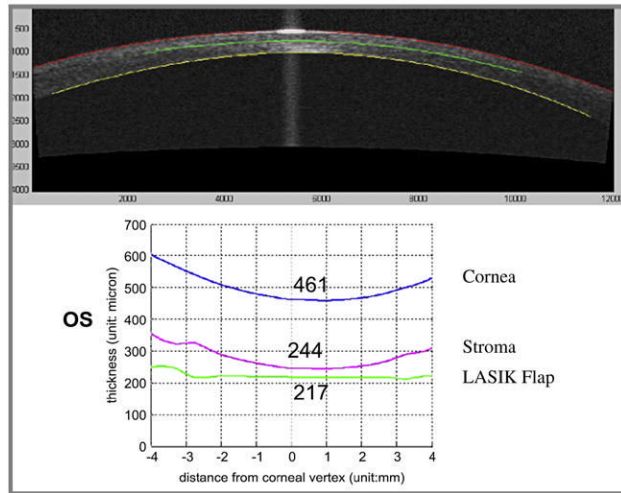


Figure 1. Case 1, right eye. A: Orbscan. B: Optical coherence tomography profile scan.



A



B

Figure 2. Case 2, left eye. A: Orbscan. B: Optical coherence tomography profile scan.

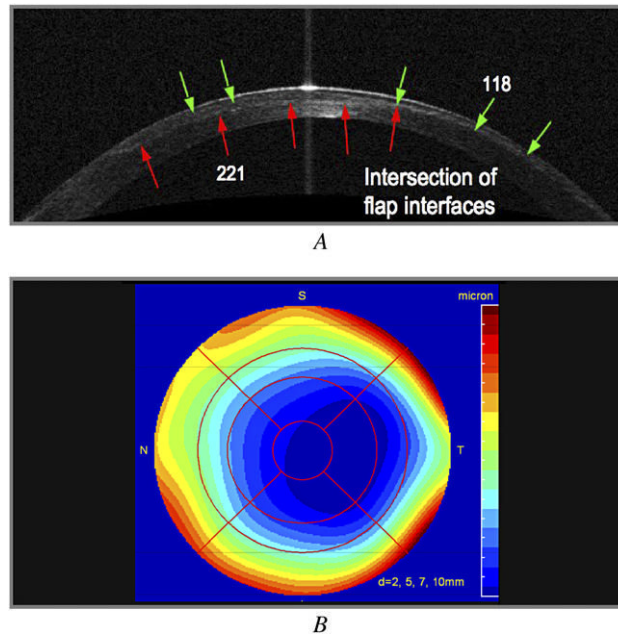


Figure 3. Case 5, left eye. *A*: Horizontal cross-sectional OCT image (red arrows = flap interface 1; green arrows = flap interface 2). *B*: Optical coherence tomography pachymetry map.

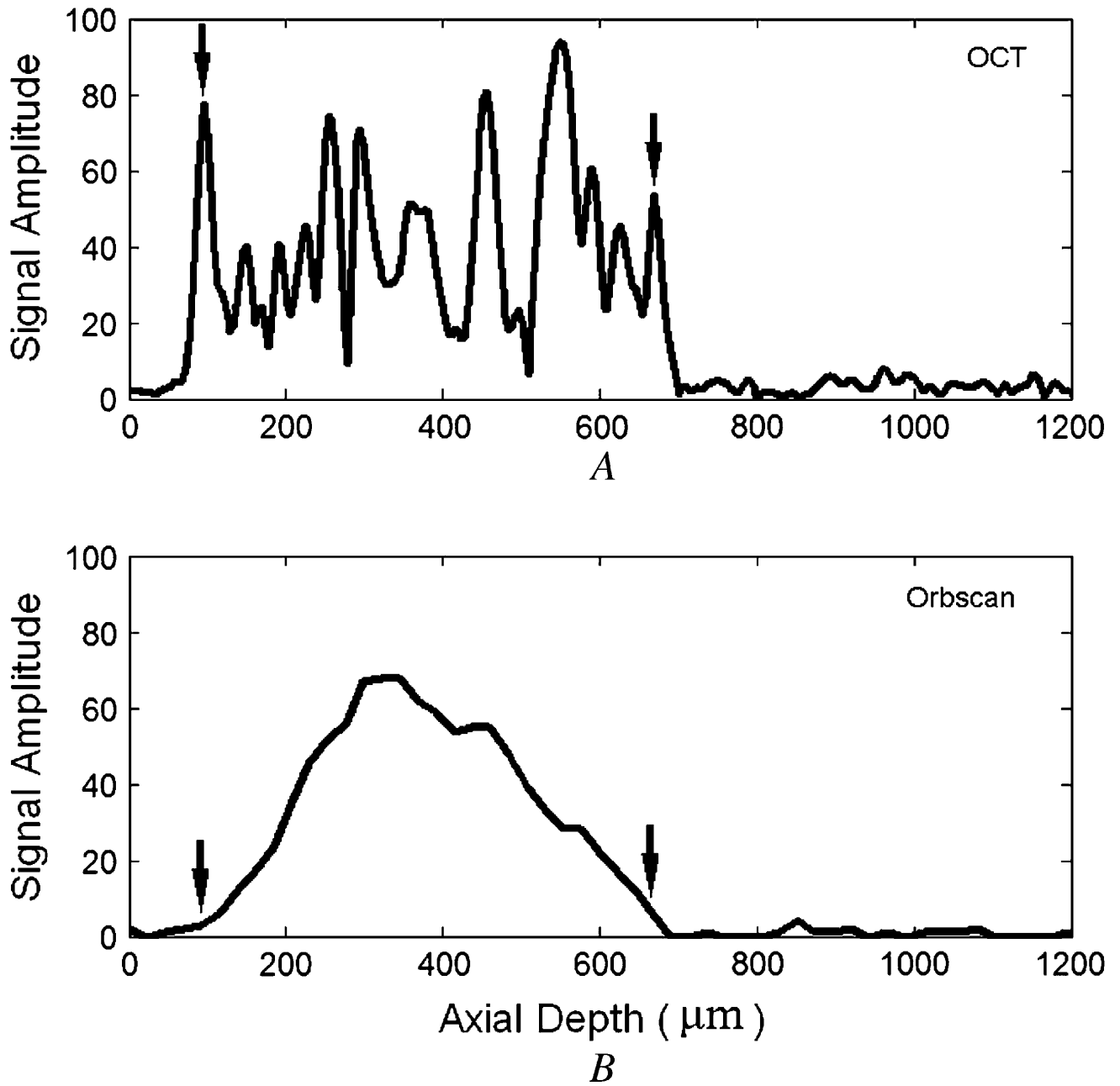


Figure 4.

Optical coherence tomography and Orbscan II A-scans. *A*: Optical coherence tomography. The anterior (*left arrow*) and posterior (*right arrow*) corneal boundaries are clearly marked by signal peaks. *B*: Orbscan II. The anterior (*left arrow*) and posterior (*right arrow*) corneal boundaries are identified by the automatic edge-processing result of Orbscan II software.

Table 1

Central thickness of post-LASIK corneal layers measured by OCT.

Case	Stromal Bed (µm)		Flap (µm)		OS	Conclusions
	OD	OS	OD	OS		
1	343	381	197	196	196	Post-LASIK posterior elevation; no keratectasia; sufficient stromal bed for enhancement
2	—	244	—	217	217	Keratectasia; insufficient residual stromal bed
3	395	375	157	181	181	Decentered hyperopic LASIK; no keratectasia; sufficient stromal bed for enhancement
4	299	299	197	194	194	Keratectasia; probable pre-LASIK forme fruste keratoconus
5	—	291	—	221	221	Loss of tissue at intersection of 2 flap cuts

LASIK = laser in situ keratomileusis

Table 2

Central corneal thickness measured by three methods.

Case	Eye	OCT (μm)	Ultrasound (μm)	Orbiscan (μm)
1	OD	540	532	336
1	OS	571	550	481
2	OS	461	454	401
3	OD	552	540	573
3	OS	556	573	569
4	OD	496	486	408
4	OS	493	408	445
5	OS	512	d	377

OCT = optical coherence tomography

The mean difference between methods—OCT versus US: $6.4 \pm 11.7 \mu\text{m}$ ($P = .17$, t test); Orbiscan versus US: $-67.5 \pm 72.5 \mu\text{m}$ ($P = .026$, t test)